Analytica Chimica Acta 1180 (2021) 338874

Contents lists available at ScienceDirect

Analytica Chimica Acta

journal homepage: www.elsevier.com/locate/aca

A targeted prenylation analysis by a combination of IT-MS and HR-MS: Identification of prenyl number, configuration, and position in different subclasses of (iso)flavonoids

Sarah van Dinteren, Carla Araya-Cloutier, Wouter J.C. de Bruijn, Jean-Paul Vincken*

Laboratory of Food Chemistry, Wageningen University, P.O. Box 17, 6700 AA, Wageningen, the Netherlands

HIGHLIGHTS

- MS fragmentation-based guideline identifies prenylated (iso)flavonoids in extracts.
- 1,1-Dimethylallyl prenylation annotated with neutral losses 42 and 68 u in IT-MS^2.
- A- or B-ring prenylation is identified by RDA fragment analysis.
- Prenyl position (*C6* or *C8*) is identified by the ratio $[M + H{-}C_4H_8]^+/[M{+}H]^+$.
- High resolution MS provides new insights in prenyl-associated fragments.

GRAPHICAL ABSTRACT

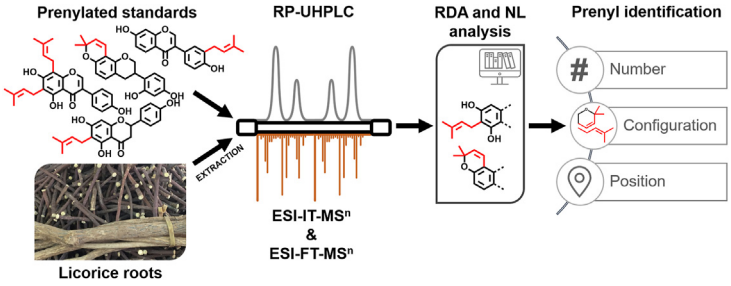

ARTICLE INFO

Article history:
Received 16 April 2021
Received in revised form
19 July 2021
Accepted 22 July 2021
Available online 26 July 2021

Keywords:
Five-carbon isoprenoid
3,3-dimethylallyl
2,2-dimethylpyran
Licorice
Glycyrrhiza glabra
Prenylation decision guideline

ABSTRACT

Prenylated (iso)flavonoids are potent bioactive compounds found in the *Fabaceae* family. Analysis and quantification of this type of phytochemicals is challenging due to their large structural diversity. In this study, the fragmentation of prenylated (iso)flavonoids was investigated using electrospray ionization ion trap mass spectrometry (ESI-IT-MS^n) with fragmentation by collision induced dissociation (CID) in combination and Orbitrap-MS (ESI-FT-MS^2) with fragmentation by higher energy C-trap dissociation (HCD). With this combination of IT-MS^n and high resolution MS (FT-MS^n), it was possible to determine the fragmentation pathways and characteristic spectral features of different subclasses of prenylated (iso) flavonoid standards, as well as characteristic fragmentations and neutral losses of different prenyl configurations. Based on our findings, a decision guideline was developed to (i) identify (iso)flavonoid backbones, (ii) annotate prenyl number, (iii) configuration, and (iv) position of unknown prenylated (iso) flavonoids, in complex plant extracts. In this guideline, structural characteristics were identified based on: (i) UV absorbance of the compound, (ii) mass-to-charge (*m/z*) ratio of the parent compound; (iii) ratio of relative abundances between neutral losses 42 and 56 u in MS^n; (iv) *retro*-Diels-Alder (RDA) fragments, neutral losses 54 and 68 u, and the ratio $[M{+}H{-}C_4H_8]^+/[M{+}H]^+$. Using this guideline, 196 prenylated (iso)flavonoids were annotated in a *Glycyrrhiza glabra* root extract. In total, 75 skeletons were

Abbreviations: RP-UHPLC-PDA-ESI-IT-MS, reversed phase ultra-high performance liquid chromatography with photo diode array detection coupled in-line to electrospray ionization ion trap mass spectrometry; FT-MS, Fourier transform mass spectrometry; PI, positive ionization; NI, negative ionization; FA, formic acid; NL, neutral loss; 1,1-DMA, 1,1-dimethylallyl; 3,3-DMA, 3,3-dimethylallyl; 2,2-DMP, 2,2-dimethylpyran; 2″-IPF, 2″-isopropenylfuran.

* Corresponding author.
E-mail address: jean-paul.vincken@wur.nl (J.-P. Vincken).

https://doi.org/10.1016/j.aca.2021.338874

single prenylated, 104 were double prenylated, and for merely 17 skeletons prenyl number could not unambiguously be annotated. Our prenylation guideline allows rapid screening for identification of prenylated (iso)flavonoids, including prenyl number, configuration, and position, in complex plant extracts. This guideline supports research on these bioactive compounds in the areas of plant metabolomics and natural products.

1. Introduction

(Iso)flavonoid metabolite profiling in complex crude plant extracts is classically performed with a combination of liquid chromatography (LC) with mass spectrometry (MS), and relies on comparisons with standard compounds and a search in databases and literature. This involves comparing obtained MS information (*e.g.* parent ions, neutral losses (NLs)) with those of previously isolated and analyzed compounds [1–4]. However, annotations are often tentative, as well-curated databases are not widely available and standards are often not commercially available [5]. Therefore, annotation of these secondary metabolites in complex matrices (such as plant extracts) with LC-MS is still a bottle-neck. In recent years, advanced state-of-the-art metabolite profiling and data analyses methods based on *e.g.* integrating both LC-MS and nuclear magnetic resonance (NMR) spectroscopy profiling have emerged, enabling unambiguous full characterization of secondary metabolites, including (iso)flavonoids in complex matrices [5,6]. Additionally, LC with high resolution MS profiling provides more in-depth metabolite identification, as it enables rapid assignment of elemental formulas to the molecular ions and all fragment ions derived thereof [7]. A major drawback of some of these state-of-the-art metabolite profiling methods is their high cost and limited availability in most (research) laboratories; therefore, techniques with broader applicability in phytochemistry research are needed. Moreover, these state-of-the-art studies have focused on *i.a.* analysis of flavonoid glycoconjugates [8] and flavonoid aglycones [7,9], and not specifically on prenylated (iso)flavonoids.

Substitution of a prenyl (3-methyl-2-butene) group on (iso)flavonoids is a ubiquitous feature in the *Fabaceae* family [10], as well in plants from *i.a.* the *Asteraceae*, *Cannabaceae*, and *Moraceae* family (Fig. 1A) [11,12]. Addition of a prenyl group alters the bioactivity of (iso)flavonoids, generally resulting in enhancement of *e.g.* antimicrobial activity [13]. Prenyl groups can possess different configurations. Firstly, they can occur as chains, *e.g.* 3,3-dimethylallyl (3,3-DMA) and 1,1-dimethylallyl (1,1-DMA). Secondly, they can be cyclized with an adjacent hydroxyl group to form rings, including six-membered rings (*e.g.* 2,2-dimethylpyran (2,2-DMP)) and five-membered rings (*e.g.* 2″-isopropenylfuran (2″-IPF)) [14,15]. Prenyl groups can be further modified with hydroxyl groups and different unsaturation patterns [16,17]. In *Glycyrrhiza* (*Fabaceae*), prenyl substitutions have been reported on various subclasses of chalcones and (iso)flavonoids, including flavanones, flavones, isoflavones, isoflavanones (Fig. 1B) [18]. So far, more than a thousand prenylated (iso)flavonoids have been identified from plants [17]. A quick PubChem search for 3,3-DMA and 2,2-DMP prenylated (iso)flavonoids revealed approximately 2000 and 700 compounds for aforementioned prenylations, respectively (Fig. 1C). This shows that prenylated (iso)flavonoids are important secondary metabolites, and tools that could assist their annotation in complex plant extracts could speed up studies in the areas of plant metabolomics and natural products. In this respect, LC with ion trap (IT) MS is a versatile and cost-effective general-purpose tool that is widely used in secondary metabolite identification [19].

Commonly, separation and identification of prenylated (iso)flavonoids in complex plant extracts is performed with a combination of LC with UV–Vis spectroscopy and electrospray ionization (ESI) MS. MS identification of (iso)flavonoids is possible in positive (PI) and negative ionization (NI) modes, based on (i) their specific fragmentation pattern and (ii) NL screening [1–4,20]. Fragmentation of (iso)flavonoids is characterized by the *retro*-Diels-Alder (RDA) reaction in which the C-ring of the (iso)flavonoid is cleaved, resulting in characteristic A- and B-ring fragment ions that provide information on the number and type of substituents of these rings (Fig. 1D). RDA fragments are also useful for identification of prenylation, as it has previously been observed that fragments $^{i,j}A^+$–prenyl moiety and $^{i,j}B^+$–prenyl moiety are indicative for A- or B-ring prenylation, respectively [1,21]. It is favorable to perform fragmentation in PI mode, as cleavage of the C-ring of isoflavones is often limited or not observed in NI mode [22]. From previous research, a few specific spectral features in relation to prenylation are known; in PI mode NLs of 56 and 68 u are associated with cleavage of a 3,3-DMA prenyl substituent upon fragmentation, whereas NLs of 15, 42, and 54 u are associated with 2,2-DMP prenylation [20,23–25]. Additionally, Simons et al. established a screening method for identification of prenyl configuration (3,3-DMA chain vs. 2,2-DMP ring) based on the ions corresponding to NLs of 42 and 56 u; a main loss of 56 u indicates chain prenylation and a main loss of 42 u indicates ring prenylation [20]. Moreover, recently it was cautiously proposed that the position of 3,3-DMA prenylation in isoflavones could be determined with NLs of 84 and 98 u, where a major NL of 84 u indicated prenylation on *C6*, and a major NL of 98 u indicated prenylation on *C8* [21]. It was also proposed that the position of 2,2-DMP prenylation in isoflavones can be putatively assigned based on characteristic NLs; a loss of 54 u with >20% relative abundance was characteristic for prenylation on *C6*, whereas a loss of 54 u with <5% relative abundance was characteristic for prenylation on *C8* [21]. However, aforementioned NLs related to prenylation have been identified with various MS ion analyzers with only a limited selection of standard compounds; Fang and co-workers [23] and Xu et al. [24] used quadrupole time of flight MS (Q-TOF-MS) and included 15 and 12 standards, respectively, whereas Zhang and co-workers [25], Simons et al. [20], and Aisyah et al. [21] used ion trap MS (IT-MS) with 10, 1, and 2 standard compounds, respectively. An overview of prior research is shown in Table 1 and Table S1. From Table 1, it is observed that fragmentation in IT-MS and Q-TOF-MS lead to different NLs as a result of differences in the fragmentation mechanisms of Q-CID and IT-CID; IT-MS^2 mainly gives NLs 42 and 56 u, whereas Q-TOF-MS^2 yields additional NLs of 15, 54, and 68 u. Even though this literature provides a starting point about characteristic spectral information on identification of prenyl configuration in (iso)flavonoids and prenyl position in isoflavones by MS, little is known about (i) if NLs of 42 and 56 u can be used to detect other prenyl configurations (besides 3,3-DMA and 2,2-DMP prenylation), (ii) rapid identification of single or double prenylation in (iso)flavonoids, and (iii) identification of prenyl position on other (iso)flavonoid backbones, besides the isoflavone subclass.

In this work, we elucidated characteristic spectral features related to prenylation and based on this, we developed a targeted

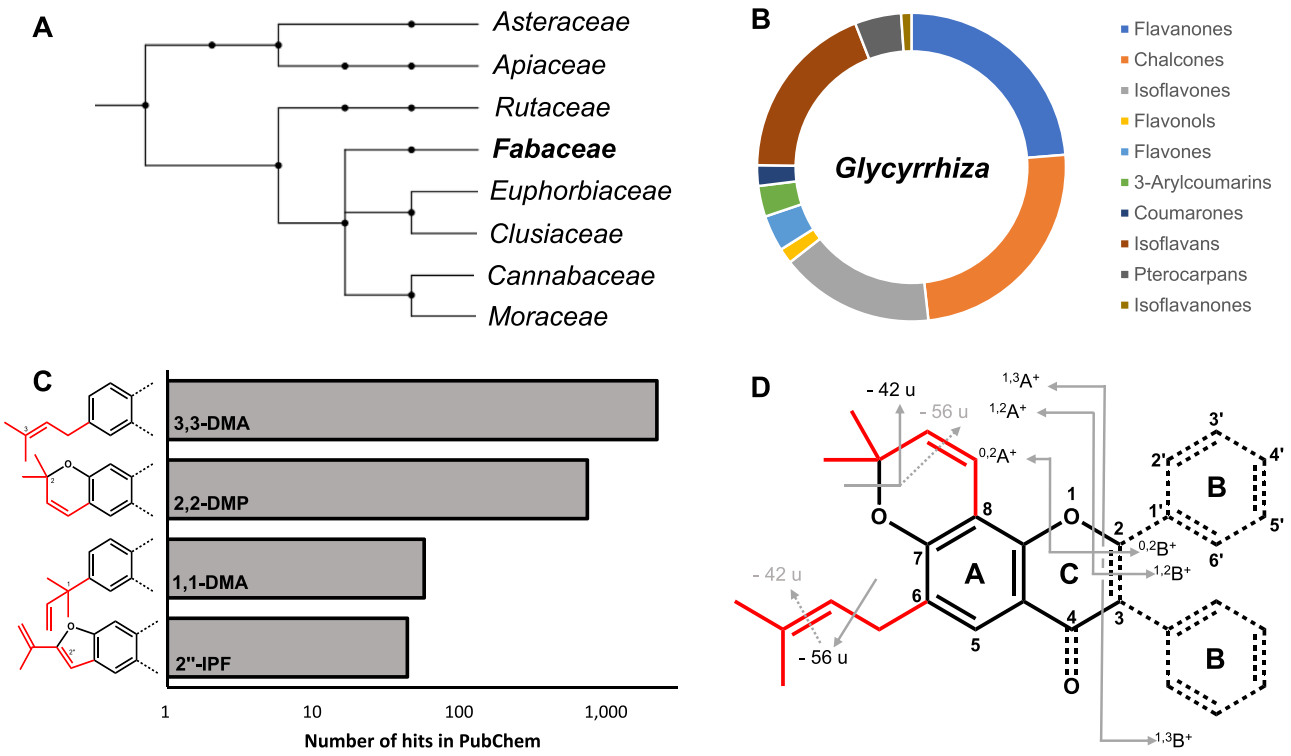

Fig. 1. Prenylation (**A**) identified in various plant families, as adapted from phyloT v2 generator, with the *Fabaceae* the most predominant family, (**B**) identified in (iso)flavonoid subclasses of *Glycyrrhiza*, adapted from Song et al. [18], (**C**) main configurations of prenyl groups on (iso)flavonoids, as retrieved from PubChem, and (**D**) common *retro*-Diels Alder (RDA) and prenyl fragmentations of (iso)flavonoids. Prenyl groups are indicated in red. The corresponding notations $^{i,j}A^+$ and $^{i,j}B^+$ are shown, where the superscripts i and j represent the bonds that are cleaved. Common cleavages with 3,3-dimethylallyl (3,3-DMA) chain and 2,2-dimethylpyran (2,2-DMP) prenylation are also shown. Solid and dashed arrows indicate major and minor cleavage sites, respectively. 1,1-DMA = 1,1-dimethylallyl and 2″-IPF = 2″-isopropenylfuran. (For interpretation of the references to colour in this figure legend, the reader is referred to the Web version of this article.)

prenylation guideline that annotates prenyl configuration, prenyl number, and prenyl position on different (iso)flavonoids backbones. For this, we systematically approached the mass spectrometric analysis of 23 prenylated (iso)flavonoid standards (Fig. S1) from different (iso)flavonoid subclasses with different number and prenyl configurations (*i.a.* 3,3-DMA, 2,2-DMP, 1,1-DMA 2″-IPF; the last two being analyzed for the first time in this study). We specifically aimed te develop a widely applicable guideline that can be used with the widely available technique IT-MS, to rapidly annotate prenylation in complex plant extracts. For this purpose, a combination of LC with UV–Vis spectroscopy, coupled to ESI-IT-MS with CID fragmentation was used. Additionally, we employed high-resolution Orbitrap-MS (ESI-FT-MS) with higher collisional dissociation (HCD) for confirmation of elemental formulas of molecular ions and fragments. As a proof of concept, compositional analysis of prenylated (iso)flavonoids in an extract of *Glycyrrhiza glabra* roots was performed. We hypothesized that prenylated (iso)flavonoids can be identified in complex crude plant extracts based on common spectral features; (i) prenyl number can be defined by the *m/z* of the parent compound, (ii) prenyl configuration can be defined by the ratio of relative abundances of NLs 42 and 56 u in MS^n, (iii) performing FT-MS^2 analyses to confirm elemental formulas of prenyl-related fragments can be used to ascertain prenyl configuration, and (iv) prenyl position (A-ring or B-ring prenylation) can be defined by analysis of RDA fragments upon fragmentation.

2. Materials and methods

2.1. Plant material and chemicals

Licorice roots, *Glycyrrhiza glabra*, were provided by Ruitenberg BasIQs BV (Twello, The Netherlands). Glabridin (≥97.0%) was purchased from Wako (Osaka, Japan); licochalcone A (≥96.0%), 6-prenylnaringenin (≥95.0%), 8-prenylnaringenin (≥95.0%), and *tert*-butanol ≥98% (w/w) from Sigma-Aldrich (St. Louis, MO, USA); glycycoumarin (≥98.0%), bavachinin (≥98.0%), and glyasperin C (≥98.0%) from ChemFaces (Wuhan, China); luteone, 2,3-dehydrokievitone, neobavaisoflavone, wighteone, lupiwighteone, isowighteone, and 6,8-diprenylgenistein from Plantech UK (Reading, UK); 6′-prenylpiscidone (≥95.0%) from Carbosynth (Compton, UK); glabrene, glabrol, hispaglabridin A, hispaglabridin B, glyceofuran, glyceollin III, and glyceollin V (all ≥95.0%, based on ^{1}H NMR) were purified previously in our laboratory [26]; ULC-MS grade ethyl acetate (EtOAc), methanol (MeOH), acetonitrile (ACN), ACN containing 0.1% (*v/v*) formic acid (FA), water containing 0.1% (*v/v*) FA, and were purchased from Biosolve (Valkenswaard, The Netherlands). Water for other purposes than UHPLC was prepared using a Milli-Q water purification system (Merck Millipore, Billerica, MA, USA).

2.2. Sample preparation and extraction

Licorice roots were freeze dried prior to milling. Roots were milled in a Retsch SM 2000 (Retsch, Haan, Germany) and subsequently sieved (pore size 250 μm, Retsch) to yield root powder. The resulting powder was extracted via ultrasound-assisted extraction with EtOAc (1:25 [*w:w*]) in 3 consecutive cycles of 15 min/cycle at 35 °C and the supernatants (after centrifugation for 20 min at 4,696 *g* at RT) of all three cycles were combined to yield the root extract. EtOAc in the root extract was removed under reduced pressure and dried extract was resolubilized in *tert*-butanol and freeze-dried. Prior to UHPLC-MS analysis, the dried root extract was resolubilized in MeOH to a final concentration of 0.1 mg mL^{-1} for ESI-FT-MS^n or

Table 1
Characteristic neutral losses related to prenyl configuration and position, reported for different MS ion analyzers in positive ionization mode.

	Reference	Fang et al. (2016)		Xu et al. (2012)			Zhang et al. (2008)		Simons et al. (2009)		Aisyah et al. (2016)		
	Plant	*Glycyrrhiza* spp.		*Psoralea corylifolia*			*Sophora flavescens*		*G. glabra*		*Lupinus* spp.		
	Interface MS	ESI		ESI			ESI		ESI		ESI		
	I.A.	Q-TOF		Q-TOF			IT		IT		IT		
	F.M.	CID		CID			CID		CID		CID		
Neutral losses	Configuration	3,3	2,2	3,3	2,2	2,2	3,3	2,2	3,3	2,2	3,3		2,2
		DMA	DMP	DMA	DMP	D3HDP	DMA	DMP	DMA	DMP	DMA		DMP
	15				✓								✓
	16				✓								
	18					✓							
	42		✓		✓				✗✓	✓			✓
	54		✓		✓				✓				✓
	56	✓		✓			✓		✓	✓	✓		
	60												✓
	68	✓		✓									
	70		✓										
	72					✓							
	Position										C6	C8	C6 C8
	54												✓[b] ✓[c]
	84										✓		
	98											✓	

I.A. = ion analyzer; F.M. = fragmentation mechanism; Ref = reference; 3,3DMA = 3,3-dimethylallyl chain; 2,2DMP = 2,2-dimethylpyran ring; 2,2D3HDP = 2,2-dimethyl-3-hydroxy-dihydropyran ring; [b]relative abundance >20%; [c]relative abundance <5%; ✗✓ = not always observed.

1 mg mL^{-1} for ESI-IT-MS^n and centrifuged (15,000 g, 5 min, RT) prior to further analysis. Standards were dissolved in MeOH and injected (after centrifugation for 5 min, 15,000 g, RT) at 100 μg mL^{-1} for ESI-IT-MS^n analysis and 3 μg mL^{-1} for ESI-FT-MS^n analysis.

2.3. Reversed phase liquid chromatography (RP-UHPLC-PDA)

Samples were separated on a Thermo Vanquish UHPLC system (Thermo Scientific, San Jose, CA, USA) equipped with a pump, degasser, autosampler and photodiode array (PDA) detector. The flow rate was 400 μL min^{-1} at a column temperature of 45 °C. Injection volume was 1 μL. Eluents used were water acidified with 0.1% (*v*/*v*) FA (A) and acetonitrile acidified with 0.1% (*v*/*v*) FA (B). Samples were separated on an Acquity UPLC BEH C18 (150 mm × 2.1 mm, i.d. 1.7 μm) with a VanGuard (5 mm × 2.1 mm, i.d. 1.7 μm) guard column of the same material (Waters, Milford, USA). The elution program was started by running isocratically at 25% B for 1.09 min, followed by 1.09–44.69 min linear gradient to 65% B, 44.69–45.78 min linear gradient to 100% B, 45.78–51.23 min isocratically at 100% B. Eluent was adjusted to its starting conditions in 1.09 min, followed by equilibration of 5.45 min. Detection wavelengths for UV–Vis were set in a range between 190 and 680 nm.

2.4. Electrospray ionization ion trap mass spectrometry (ESI-IT-MS^n)

Mass spectrometric data were acquired using a LTQ Velos Pro linear ion trap mass spectrometer (Thermo Scientific) equipped with a heated ESI probe coupled in-line to the Vanquish UHPLC system. Nitrogen was used as sheath gas (48 arbitrary units), auxiliary gas (11 arbitrary units), and sweep gas (2 arbitrary units). Data were collected in negative ionization (NI) and positive ionization (PI) mode between *m/z* 200–1000. Based on experience with fragmentation of prenylated (iso)flavonoids in our laboratory [20,21,27,28], data dependent MS^n analyses were performed by collision-induced dissociation with a normalized collision energy of 35%. MS^n fragmentation was performed on the most intense product ion in the MS^{n-1} spectrum. Dynamic exclusion, with a repeat count of 3, repeat duration of 5.0 s and an exclusion duration of 5.0 s was used to obtain MS^2 spectra of multiple different ions present in full MS at the same time. Ion transfer tube temperature was 254 °C, source heater temperature 408 °C, and the source voltage was 3.5 (PI) and 2.5 (NI) kV. Data were processed using Xcalibur 4.1 (Thermo Scientific).

2.5. Electrospray ionization hybrid quadrupole Orbitrap mass spectrometry (ESI-FT-MS)

Accurate mass data were acquired using a Thermo Q Exactive Focus hybrid quadrupole-Orbitrap Fourier transform mass spectrometer (FT-MS) (Thermo Scientific) equipped with a heated ESI probe. Samples were separated on a Vanquish UHPLC system (Thermo Scientific), as described above. Prior to analysis, the mass spectrometer was calibrated in PI and NI mode using Tune 2.11 (Thermo Scientific) by injection of Pierce negative and positive ion calibration solutions (Thermo Scientific). Used gas flows and source conditions were the same as for ESI-IT-MS. Full MS and higher energy C-trap dissociation (HCD) fragmentation data were recorded at 70,000 and 35,000 resolution, respectively. Normalized collision energy was 35%. MS^n fragmentation was performed on the most intense product ion in the MS^{n-1} spectrum. Data were processed using Xcalibur 4.1 (Thermo Scientific).

2.6. Quantification of prenylated (iso)flavonoids in licorice extract

Quantification of (iso)flavonoids was based on UV absorbance at 280 nm. For this, a six-point (0.2–100 μg mL^{-1}) calibration curve based on an external standard of glabridin ($R^2 = 0.999$) was used. Subsequently, content of each compound was corrected for the differences in molar extinction coefficients between the standard and the compounds of interest, using a derivative of Lambert-Beer's law (Eq. (1)).

$$\varepsilon_{Glab} C_{Glab} = \varepsilon_X C_X \quad (1)$$

In which ε (AU/M·cm at 280 nm) is the molar extinction coefficient, C is the molar concentration, Glab is glabridin, and X is the (iso)flavonoid to be quantified. Concentrations of compounds were recalculated to μg per g of dry weight (DW) of the licorice root powder (μg g^{-1} DW). See Table S2 for an overview of the molar extinction coefficients used for these calculations [26,27,29,30].

3. Results and discussion

3.1. Spectral properties of prenylated (iso)flavonoids

A diverse set of 24 standards was selected (Fig. S1), which included different (iso)flavonoid subclasses (isoflavan, isoflavone, isoflav-3-ene, 3-arylcoumarin, pterocarpan, flavanone, chalcone), and various prenyl configurations (chain, furan, and pyran) and positions (*C3'*, *C6'*, *C6*, and *C8*). In the paragraphs below, all standards are discussed with respect to their UV absorbance and parent *m/z*, their characteristic NLs associated with the prenyl moiety, and their RDA fragments and specific NLs associated with prenyl position. An overview of all obtained spectrometric data (UV, NI and PI mode with IT-MS^n and FT-MS^n) of standards is listed in Table S5.

3.1.1. (Iso)flavonoid subclass, presence, and number of prenylation

UV absorbance spectra of all standards complied with the (iso)flavonoid subclass specific UV absorbances known from literature; for example, glabridin (isoflavan) showed a maximum UV absorbance at 278 nm, which is in agreement with the typical UV absorbance of isoflavans, which was reported to be between 270 and 285 nm [31], whereas licochalcone A (chalcone) showed a maximum UV absorbance at 378 nm corresponding to the typical band I absorption of chalcones between 340 and 390 nm [32]. Based on our results (Table S3) and previously reported spectral data [33,34], we propose to use a UV absorbance cut-off of at least 240 nm as a first criterion to identify potential (prenylated) (iso)flavonoids. Next, *m/z* ratios of the parent ions of all standards were compiled; *m/z* ratios in PI ranged from 323 for glabrene (single prenylated isoflav-3-ene) to 453 for 6′-prenylpiscidone (double prenylated isoflavone) (Table S5). The smallest natural prenylated flavonoid is 7,8-(2,2-dimethylchromeno) flavone, with a molecular weight of 304 g mol^{-1} ($C_{20}H_{16}O_3$) [14,35,36]. Thus, a second criterion was defined based on parent *m/z* of the compound; *m/z* ratio of the parent molecule in PI mode <305 indicates a non-prenylated (iso)flavonoid, *m/z* of 305–373 indicates a single prenylated (iso)flavonoid, and *m/z* >373 (305+68) indicates a double prenylated (iso)flavonoid.

3.1.2. Prenyl configuration

All standards were screened for the presence of ions in IT-MS^n that corresponded to NLs of 42 and 56 u. An overview of these NLs, with their relative abundances, is shown in Table S3; all compounds' IT-MS^2, IT-MS^3, and FT-MS^2 spectra in PI mode are shown in Figs. 2, 3, and 4, and Figs. S2 and S3. With the previously established prenyl configuration rule by Simons et al. [20] (a ratio of NLs 56:42 >1 indicative for 3,3-DMA prenylation and <1 indicative for 2,2-DMP prenylation), prenyl configuration of all standards was identified; the ratio of the relative abundances of the ions corresponding to NLs of 42 and 56 u correctly identified 3,3-DMA and 2,2-DMP prenylation in all tested standards.

For example, IT-MS^2 fragmentation of the 3,3-DMA prenylated genistein (isoflavone) derivatives isowighteone, wighteone, lupiwighteone, and 6,8-diprenylgenistein, showed a main fragment at $[M+H-C_4H_8]^+$ (*m/z* 283 for isowighteone, wighteone, and lupiwighteone, and *m/z* 351 for 6,8-diprenylgenistein), corresponding to a NL of 56 u (Fig. 2A1). Double prenylation in 6,8-diprenylgenistein was confirmed by IT-MS^3 fragmentation on fragment $[M+H-C_4H_8]^+$, yielding fragment $[M+H-C_4H_8-C_4H_8]^+$ (*m/z* 295) (Fig. 2A2). Molecular formulas of fragments were confirmed by FT-MS^2 (Fig. 2A3). FT-MS^2 fragmentation showed a similar fragmentation pattern as IT-MS^2 with different relative intensities of fragments. Differences in relative intensities of fragments are due to the use of CID in our IT-MS^n analyses and HCD in our FT-MS^2 analyses. Additionally, HCD improves fragmentation in the low mass region [37], which can provide useful ions for confirmation and screening purposes to detect prenylated compounds based on this MS^2 fragment. It should be noted that correct identification of prenyl configuration by the ratio of the relative abundances of the ions corresponding to NLs 42 and 56 u was instrument dependent, as it was correctly identified by IT-MS^n and not always by HR-MS^2.

2,2-DMP prenylation in glabrene (isoflav-3-ene) was confirmed with IT-MS^2 (56:42 <1, relative abundance *m/z* 267 < *m/z* 281) (Fig. S2D1). Fragmentation of glabrene showed an intense fragment at *m/z* 279 in IT-MS^2 that possessed a molecular formula of $C_{17}H_{11}O_4^+$ (based on FT-MS^2, Δ-0.88 ppm, Fig. S2D3), and corresponded to neutral loss of 44 u (C_3H_8). A fragment with this NL was only observed in glabrene and could be a subclass (*i.e.* isoflav-3-ene) specific prenyl-related fragment. For several other 2,2-DMP prenylated isoflavan standards, including glabridin (Fig. 3A2), hispaglabridin A (Fig. S2A2), and hispaglabridin B (Fig. S2B2), IT-MS^3 fragmentation was required to confirm 2,2-DMP prenylation with RDA fragment $^{1,3}A^+-C_3H_6$ (fragments at *m/z* 147, 161, and 147, respectively). Aforementioned fragments also provided information on prenyl position, as the NL associated with the prenyl moiety (C_3H_6) was seen on the A-ring fragment.

An interesting result was that the ratio of the relative abundances of the ions corresponding to NLs 42 and 56 u did not correctly identify 1,1-DMA prenylation (licochalcone A) and furan ring prenylation (pterocarpans glyceollin V and glyceofuran). For these compounds, high resolution MS^2 was required to identify molecular formulas of fragments. IT-MS^2 fragmentation of licochalcone A showed a major fragment at *m/z* 297 (NL of 42 u) and a minor fragment at *m/z* 283 (NL of 56 u) (Fig. 3B1). The ratio 56:42 <1 suggested 2,2-DMP prenylation, however, FT-MS^2 (Fig. 3B3) indicated that the molecular formula of *m/z* 297.14890 was $C_{19}H_{21}O_3^+$ (Δ1.27 ppm), which corresponded to loss of C_2H_2O (ketene). This ketene loss was reported in literature as a result of Nazarov cyclization of 2-methoxychalcones or 2′-hydroxychalcones during CID, which mediates proton transfer and subsequent fragmentation with a loss of a ketene (Fig. S4) [38,39]. Fragment ion *m/z* 271 $[M+H-C_5H_8]^+$ in IT-MS^2 in combination with fragment ion *m/z* 69.07011 ($C_5H_9^+$, Δ3.37 ppm) in FT-MS^2 were crucial for correct identification of 1,1-DMA prenylation in licochalcone A (Fig. 3B1 and B.3). Observation of *m/z* 69 indicates that for 1,1-DMA prenylation, the whole prenyl chain is cleaved off [23–25]. In our analyses, fragment *m/z* 69 was detected in FT-MS^2 with HCD, but it should be noted that detection of fragment *m/z* 69 can also be achieved with CID by lowering the activation Q or using pulsed Q CID (PQD), thereby circumventing the "1/3rd rule" [40].

Next, fragmentation behavior of furan ring prenylated pterocarpans glyceollin III (6,7-(2″-isopropenyldihydrofuran)), glycollin V

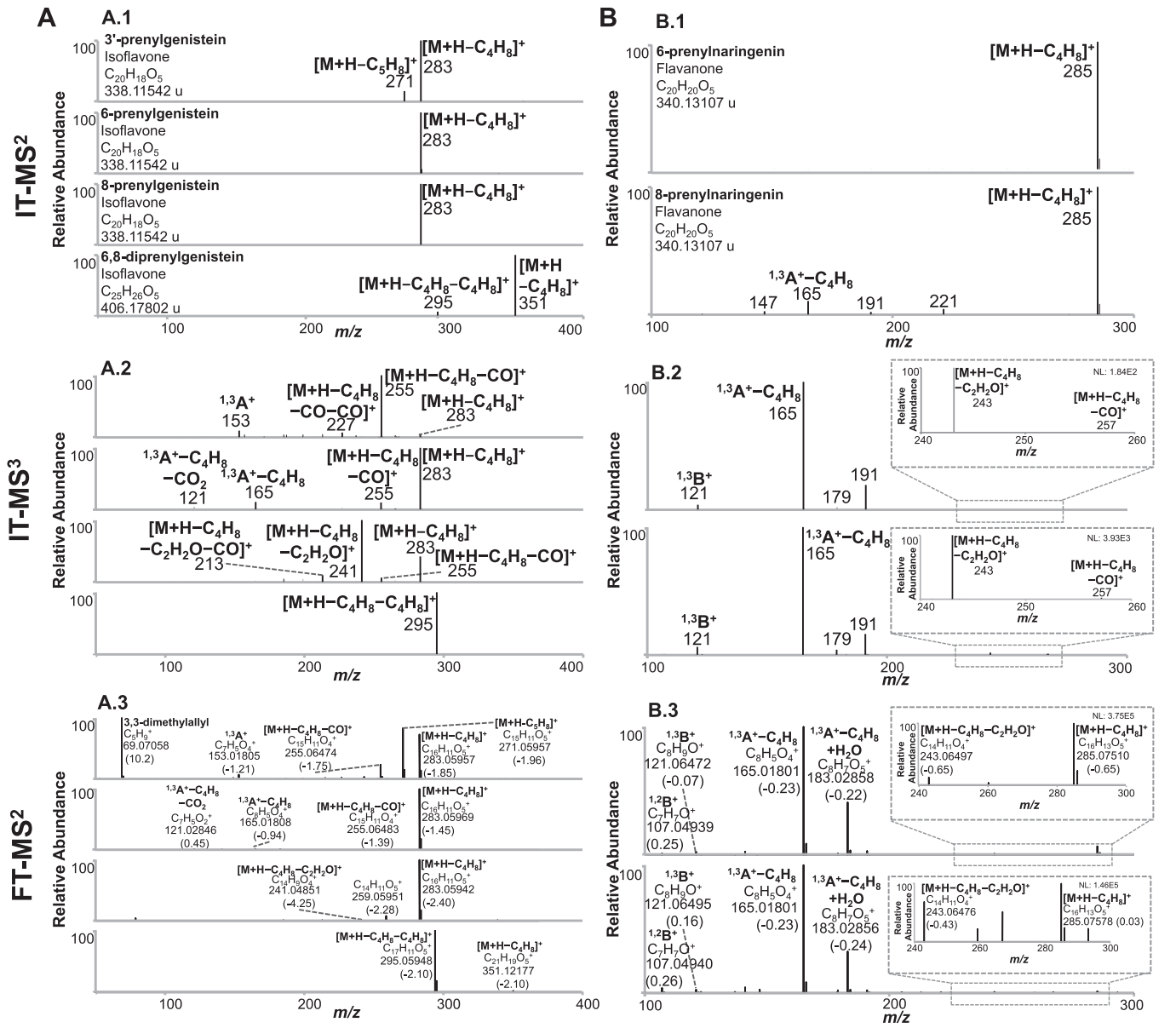

Fig. 2. Positive mode ESI-IT-MS and ESI-FT-MS fragmentation spectra (NCE = 35) of (**A**) isoflavones 3′-prenylgenistein (isowigtheone), 6-prenylgenistein (wighteone), 8-prenylgenistein (lupiwighteone), and 6,8-diprenylgenistein, (**B**) flavanones 6-prenylnaringenin and 8-prenylnaringenin. **A.1.** and **B.1.** show IT-MS^2 spectra, **A.2.** and **B.2.** IT-MS^3 spectra, and **A.3.** and **B.3.** FT-MS^2 spectra. IT-MS^3 fragmentation was performed on the most abundant fragment from IT-MS^2. Peak labels show the corresponding fragmentation pathway, fragment (with its molecular formula for FT-MS), and *m/z* (with error in ppm in parentheses). Fragments were labelled based on a cut-off value at 10% relative abundance; unless they were specific fragments used for screening (including RDA fragments, fragments associated with the prenyl). Structural formulas of compounds are shown in Table S3 (Supplementary information). (Iso)flavonoid subclass, molecular formula, and exact mass of the precursor ions are shown in **A.1** and **B.1**. In **B.2** and **B.3**, specific fragments used for screening are shown in amplified regions of the spectra, displayed in dashed boxes.

(6,7-(2″-isoproprenylfuran)), and glyceofuran (6,7-(2″-(2-hydroxy-) isopropenylfuran)) was studied to elucidate whether five-membered (furan) prenyl rings fragment similarly to six-membered (pyran) prenyl rings, as suggested by Simons and co-workers [41]. Only for glyceollin III (Fig. S2F1), the ratio of the relative abundances of the ions corresponding to NLs 42 u (*m/z* 279) and 56 u (*m/z* 265) correctly identified ring prenylation (56:42 <1). However, the NL of 56 u was not associated with the prenyl; *m/z* 265.12183 in FT-MS^2 (Fig. S2F3) matched to $C_{18}H_{17}O_2^+$ (Δ-1.80 ppm), indicating the loss of two carbonyl moieties ($M+H-H_2O-CO-CO^+$). Glyceollin V and glyceofuran showed similar fragmentation behavior where both NLs of 42 (fragments *m/z* 277 for glyceollin V and *m/z* 295 for gluceofuran) and 56 u (fragments *m/z* 263 for glyceollin V and *m/z* 281 for glyceofuran) were not associated with the prenyl (Fig. S2G and S2.H), but with losses of a ketene $[M+H-H_2O-C_2H_2O]^+$ and two carbonyl moieties $[M+H-H_2O-CO-CO]^+$, respectively. Also, the ratio 56:42 >1 incorrectly identified chain prenylation. From above results, we conclude that the ratio NLs of 42 and 56 u in IT-MS^2 cannot be used for identification of furan prenylated (iso)flavonoid compounds.

Thus, when a complex plant extract is analyzed which potentially contains novel prenylated compounds, or if it is known from literature that furan prenylated compounds may be present, it is valuable to use high resolution MS; we recommend verification of the molecular formulas of the fragment ions with high resolution MS to prevent false positive identification of 3,3-DMA prenylation. Moreover, molecular formulas obtained with high resolution MS can give insights in new compounds in complex extracts.

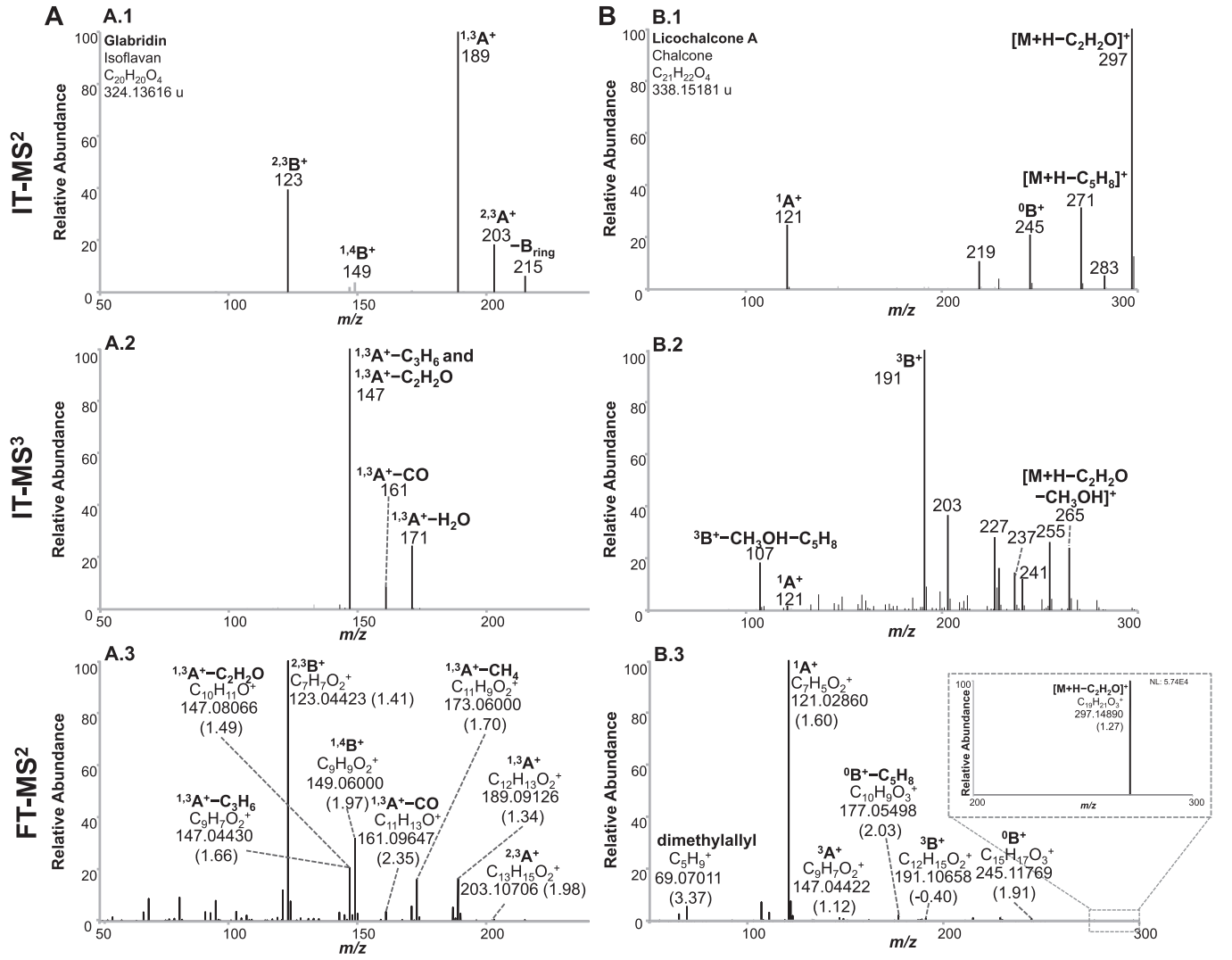

Fig. 3. Positive mode ESI-IT-MS and ESI-FT-MS fragmentation spectra (NCE = 35) of (**A**) isoflavan glabridin and (**B**) licochalcone A. **A.1.** and **B.1.** show IT-MS^2 spectra, **A.2.** and **B.2.** IT-MS^3 spectra, and **A.3.** and **B.3.** FT-MS^2 spectra. IT-MS^3 fragmentation was performed on the most abundant fragment from IT-MS^2. Peak labels show the corresponding fragmentation pathway (Figs. S6–S10, Supplementary Information), fragment (with its molecular formula for FT-MS), and *m/z* (with error in ppm in parentheses). Fragments were labelled based on a cut-off value at 10% relative abundance; unless they were specific fragments used for screening (including RDA fragments, fragments associated with the prenyl). Structural formulas of compounds are shown in Table S3 (Supplementary information). (Iso)flavonoid subclass, molecular formula, and exact mass of the precursor ions are shown in **A.1** and **B.1**. In **B.3** specific fragments used for screening are shown in amplified regions of the spectra, displayed in dashed boxes.

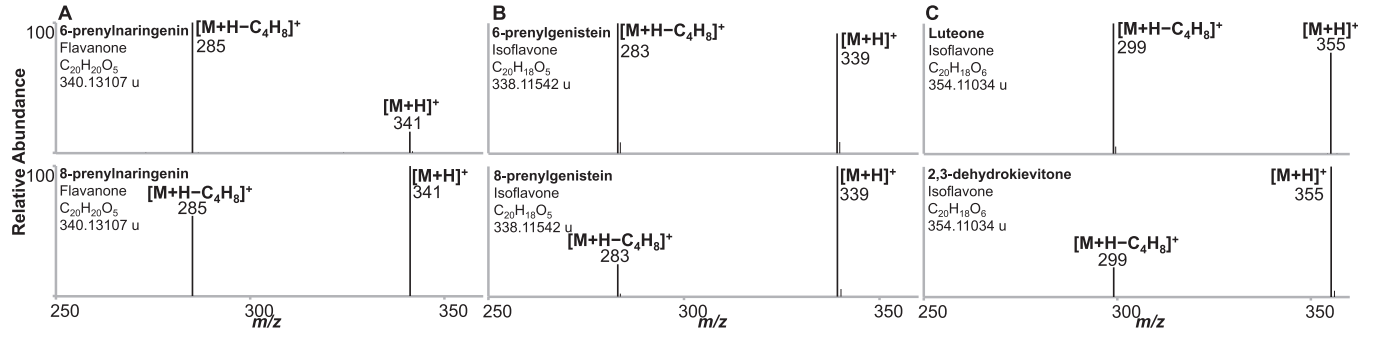

Fig. 4. Positive mode ESI-IT-MS^2 fragmentation spectra (NCE = 20) of (A) flavanones 6-prenylnaringenin (upper), 8-prenylnaringenin (lower) (B) isoflavones 6-prenylgenistein (i.e. wighteone) (upper), 8-prenylgenistein (i.e. lupiwighteone), (lower) and (C) isoflavones luteone (upper) and 2,3-dehydrokievitone (lower). Peak labels show the corresponding fragmentation pathway. Structural formulas of compounds are shown in Table S3 (Supplementary information). (Iso)flavonoid subclass, molecular formula, and exact mass of the precursor ions are shown in A, B, and C.

3.1.3. *Prenyl position*

For all tested standards, prenyl position on the (iso)flavonoid backbone (A- or B-ring) and subsequent *C6* or *C8* prenylation (for A-ring prenylated compounds) was identified based on RDA fragments

and characteristic NLs in IT-MS^n. Identification of fragments was further established with FT-MS^2 by confirmation of their molecular formulas. An overview of characteristic RDA fragments and NLs is listed in Table S3.

3.1.3.1. A- or B-ring prenylation. Based on the RDA fragments in IT-MS^n, fragments $^{i,j}A^+-$prenyl and $^{i,j}B^+-$prenyl were indicative for A- or B-ring prenylation, respectively. Molecular formulas of fragments were confirmed with FT-MS^2. A- or B-ring prenylation in all isoflavan, isoflavone, isoflav-3-ene, flavanone, chalcone, 3-arylcoumarin, and pterocarpan standards were identified correctly. For example, IT-MS^3 fragmentation of hispaglabridin A, a double prenylated isoflavan with a 2,2-DMP on the A-ring and a 3,3-DMA on the B-ring, showed fragments at *m/z* 147 and 149, corresponding to $^{1,3}A^+-C_3H_6$ and $^{1,3}B^+-C_4H_8$ (Fig. S2A2), respectively. These fragments confirmed 2,2-DMP prenylation on the A-ring and 3,3-DMA prenylation on the B-ring. Molecular formulas were confirmed with FT-MS^2 (Fig. S2A3). Our observation of fragment $^{1,3}A^+$ was in agreement with typical RDA fragments observed for isoflavans [4]. Analysis of RDA fragments did not only identify prenyl position in (iso)flavonoids, but also in chalcones; B-ring prenylation in licochalcone A was confirmed in IT-MS^2 and IT-MS^3 with fragments *m/z* 245 and *m/z* 191 (Fig. 3B1 and B.2). These fragments corresponded to RDA fragments $^0B^+$ and $^3B^+$, respectively, and were substituted with the whole 1,1-DMA prenyl chain. All molecular formulas were confirmed with FT-MS^2 (Fig. 3B3). A-ring furan prenylated pterocarpans glyceollin and glyceofuran showed RDA fragments substituted with the prenyl moiety in IT-MS^2 at *m/z* 159, 187, and 211, and in IT-MS^3 at *m/z* 173, corresponding to $^{0,4}A^+-H_2O$, $^{2,4}A^+-H_2O$, $^{5,6}A^+-H_2O$ and $^{1,4}A^+-H_2O$, respectively (Fig. S2F1 and S2F.2). Molecular formulas were confirmed with FT-MS^2 (Fig. S2F3). More detailed RDA fragmentation of pterocarpans is described by Simons and co-workers [41]. IT-MS^3 analysis of glycycoumarin (3,3-DMA chain A-ring prenylated 3-arylcoumarin) indirectly confirmed A-ring prenylation by RDA fragments $^{2,3}B^+$ (*m/z* 123) and $^{2,4}B^+$ (*m/z* 135) (Fig. S2C2 and S2C.3); only B-ring RDA fragments were detected, without substitution of a prenyl moiety. Detection of RDA fragment $^{2,4}B^+$ is in agreement with work from Waffo and co-workers [42]. Proposed RDA fragmentation pathways of glabridin, licochalcone A, glycycoumarin, hispaglabridin A, hispaglabridin B, glabrol, and glabrene are shown in Figs. S6–S10.

Next to analysis of RDA fragments to identify A- or B-ring prenylation, an interesting difference was observed between the IT-MS^2 spectra of isowighteone (*C3*' 3,3-DMA prenylated isoflavone), wighteone (*C6* 3,3-DMA prenylated isoflavone), and lupiwighteone (*C8* 3,3-DMA prenylated isoflavone). Isowighteone showed a fragment at *m/z* 271 (Fig. 2A1), which was absent in the spectra of wighteone and lupiwighteone. FT-MS^2 assigned this fragment to molecular formula $C_{15}H_{11}O_5^+$ (*m/z* 271.05957, Δ-1.96 ppm) (Fig. 2A3), suggesting the loss of the whole prenyl chain (C_5H_8, NL of 68 u) from the parent molecule. The same was observed for other *C3*' prenylated compounds, which also yielded a fragment corresponding to loss of the whole prenyl chain (licoisoflavone A (*m/z* 287), neobavaisoflavone (*m/z* 255), 6′-prenylpiscidone (*m/z* 329) in Fig. S3A1). Aforementioned results suggested that presence of fragment $[M+H-C_5H_8]^+$ in IT-MS^2 was indicative for B-ring 3,3-DMA prenylated isoflavones. However, recent evidence suggested that fragment $[M+H-C_5H_8]^+$ is the major ion of A-ring prenylated (iso)flavonoids in which the *ortho* position of the prenylated benzene is substituted with a methoxy group [24]. We therefore studied the fragmentation of bavachinin (*C6* 3,3-DMA prenylated *C7* methoxylated flavanone) and glyasperin C (*C6* 3,3-DMA prenylated *C5* methoxylated isoflavan); IT-MS^2, IT-MS^3, and FT-MS^2 spectra are shown in Fig. S2I and S2.J. Indeed, IT-MS^2 spectra of bavachinin and glyasperin C showed fragment $[M+H-C_5H_8]^+$ at *m/z* 271 (Fig. S2I.A) and *m/z* 289 (Fig. S2J.A), respectively. Molecular formulas were confirmed with FT-MS^2 (Fig. S2I.C and S2J.C). From these results we conclude that fragment $[M+H-C_5H_8]^+$ does not necessarily indicate B-ring prenylation. Interestingly, we observed another difference in IT-MS^2 fragmentation between (i) A-ring 3,3-DMA, (ii) A-ring 3,3-DMA with neighboring methoxy-group, and (iii) B-ring 3,3-DMA prenylated compounds. Compounds belonging to groups (i) and (iii) did not yield RDA fragments (or RDA fragment abundance was <10%), whereas compounds belonging to group (ii) produced RDA fragments (with >10% relative abundance). We therefore propose that fragment $[M+H-C_5H_8]^+$ in absence of RDA fragments in IT-MS^2 is diagnostic to distinguish A- or B-ring prenylation in 3,3-DMA prenylated isoflavonoids.

From above results, we conclude that analysis of RDA fragments in IT-MS^n, in combination with molecular formula confirmation by FT-MS^2, is a useful tool to identify A- or B-ring prenylation in different classes of (iso)flavonoids. Fragments $^{i,j}A^+-$prenyl and $^{i,j}B^+-$prenyl are diagnostic ions, *i.e.* fragment ion $^{i,j}A^+-C_4H_8$ or $^{i,j}B^+-C_4H_8$ confirms 3,3-DMA prenylation on the corresponding ring and fragment ion $^{i,j}A^+-C_3H_6$ or $^{i,j}B^+-C_3H_6$ serves the same purpose for 2,2-DMP prenylation. Additionally, we propose that A- or B-ring prenylation can easily be distinguished in IT-MS^2 by the presence of fragment $[M+H-C_5H_8]^+$ in combination with absence of RDA fragments in the case of B-ring 3,3-DMA prenylated isoflavones.

3.1.3.2. C6 or C8 prenylation. In a study by Aisyah and co-workers, it was proposed that NLs 84 and 98 u in IT-MS^3 can be used to identify *C6* or *C8* 3,3-DMA prenylation, respectively, whereas the relative abundance of the ion corresponding to a NL of 54 u was used to distinguish *C6* (>20% relative abundance) or *C8* (<5% relative abundance) 2,2-DMP prenylation [21]. We compared these proposed NL-related guidelines to the mass spectra of all our A-ring prenylated standards. Analysis of the relative abundance of the ion corresponding to a NL of 54 u ($[M+H-C_4H_6]^+$) in IT-MS^n correctly identified *C8* 2,2-DMP prenylation in the *C8* 2,2-DMP prenylated isoflavans glabridin, hispaglabridin A, and hispaglabridin B; fragments with a NL of 54 u were absent in IT-MS^n (Table S3). A limitation in our study was the absence of *C6* 2,2-DMP prenylated standards; we suggest to verify a NL of 54 u in IT-MS^n with authentic standards of *e.g.* parvisoflavone A (*C8* 2,2-DMP prenylated isoflavone) and parvisoflavone B (*C6* 2,2-DMP prenylated isoflavone), which were not commercially available. This could determine with more certainty if a NL of 54 u can distinguish *C6* and *C8* 2,2-DMP prenylation. For isoflavone isomers wighteone (*C6* 3,3-DMA prenylated) and lupiwighteone (*C8* 3,3-DMA prenylated), IT-MS^3 was useful to elucidate prenyl position (Table S3); lupiwighteone yielded a major ion at *m/z* 241 (NL of 98 u) (Fig. 2A2), indicating the loss of C_2H_2O from $[M+H-C_4H_8]^+$. Wighteone did not give *m/z* 241 in MS^3, instead an ion at *m/z* 255 was seen (NL of 84 u), indicating the loss of CO from $[M+H-C_4H_8]^+$. Both fragments were confirmed with FT-MS^2 (Fig. 2A3). The mechanism behind this difference in fragmentation between *C6* and *C8* prenylated isomers remains to be elucidated. However, the relative abundances of the ions corresponding to NLs of 84 and 98 u in IT-MS^3 did not always correctly identify *C6* and *C8* 3,3-DMA prenylation (Table S3). Incorrect identification did not seem to be subclass specific, as this was observed for both isoflavone and flavanone standards; the IT-MS^3 spectra of luteone (*C6* 3,3-DMA prenylated isoflavone) and 6-prenylnaringenin (*C6* 3,3-DMA prenylated flavanone) showed minor NLs (with <1% relative abundance) of 84 and 98 u with similar intensities (Fig. S3A2 and Fig. 2B2), making it impossible to confirm *C6* prenylation.

In order to correctly identify *C6* or *C8* 3,3-DMA prenylation, we tested fragmentation of the standard compounds with lower normalized collision energies (NCE 15, 20, 25, and 35) (Fig. 4). It was shown previously that 8-prenylated flavanones were less likely to lose C_4H_8 during fragmentation than their 6-prenylated isomers

[43,44]. Indeed, when we lowered the NCE from 35 to 20, the relative abundance of fragment $[M+H-C_4H_8]^+$ of the 6- and 8-prenylated isomers changed differentially for all tested standards, making them easily distinguishable in IT-MS^2. For example, 6-prenylnaringenin (Fig. 4A) readily lost its C_4H_8 moiety and yielded fragment $[M+H-C_4H_8]^+$ at *m/z* 285 with 100% relative abundance, whereas 8-prenylnaringenin showed parent ion $[M+H]^+$ at *m/z* 341 with 100% relative abundance and fragment $[M+H-C_4H_8]^+$ with 62% relative abundance. Isoflavones isowighteone, lupiwighteone, luteone, and 2,3-dehydrokievitone showed similar fragmentation behavior (Fig. 4B and C). Based on these results, we formulated a new rule of differentiating between *C6* and *C8* 3,3-DMA prenylation; if the relative abundance of $[M+H]^+$ is lower than the relative abundance of $[M+H-C_4H_8]^+$ (at low NCE) then the molecule is *C6* prenylated, whereas if the relative abundance of $[M+H]^+$ is higher than $[M+H-C_4H_8]^+$ then the molecule is *C8* prenylated. The underlying reason for this difference in relative abundance of fragment $[M+H-C_4H_8]^+$ in IT-MS^2 between *C6* and *C8* prenylated isomers is still unknown. It could be hypothesized that the hydroxyl groups adjacent to the prenyl moiety at *C6* make the prenyl moiety a better leaving group; the *C6* chain prenylated compounds (wighteone, luteone, and 6-prenylnaringenin) have two *ortho* phenolic hydroxyl groups present adjacent to the prenyl, whereas the *C8* chain prenylated compounds (lupiwighteone, 2,3-dehydrokievitone and 8-prenylnaringenin) have only one. Moreover, when applying this new rule, we recommend optimization of the NCE and the required reduction in NCE for each individual MS system, as the actual CID energy will differ between instruments and may even change over time.

3.2. Decision guideline for identification of prenylation configuration, number, and position in (iso)flavonoids

Based on the characteristic spectral properties of prenylated (iso)flavonoid standards (Section 3.1.), a decision guideline was developed in order to quickly identify prenyl number, configuration (Fig. 5A), and position (Fig. 5B and C) in (iso)flavonoids. Our guideline can be used as follows; when starting at the upper arrow (Fig. 5A), the first criterion is based on UV absorbance (Fig. 5A, "UV absorbance); if the compound has a UV absorbance >240 nm, the

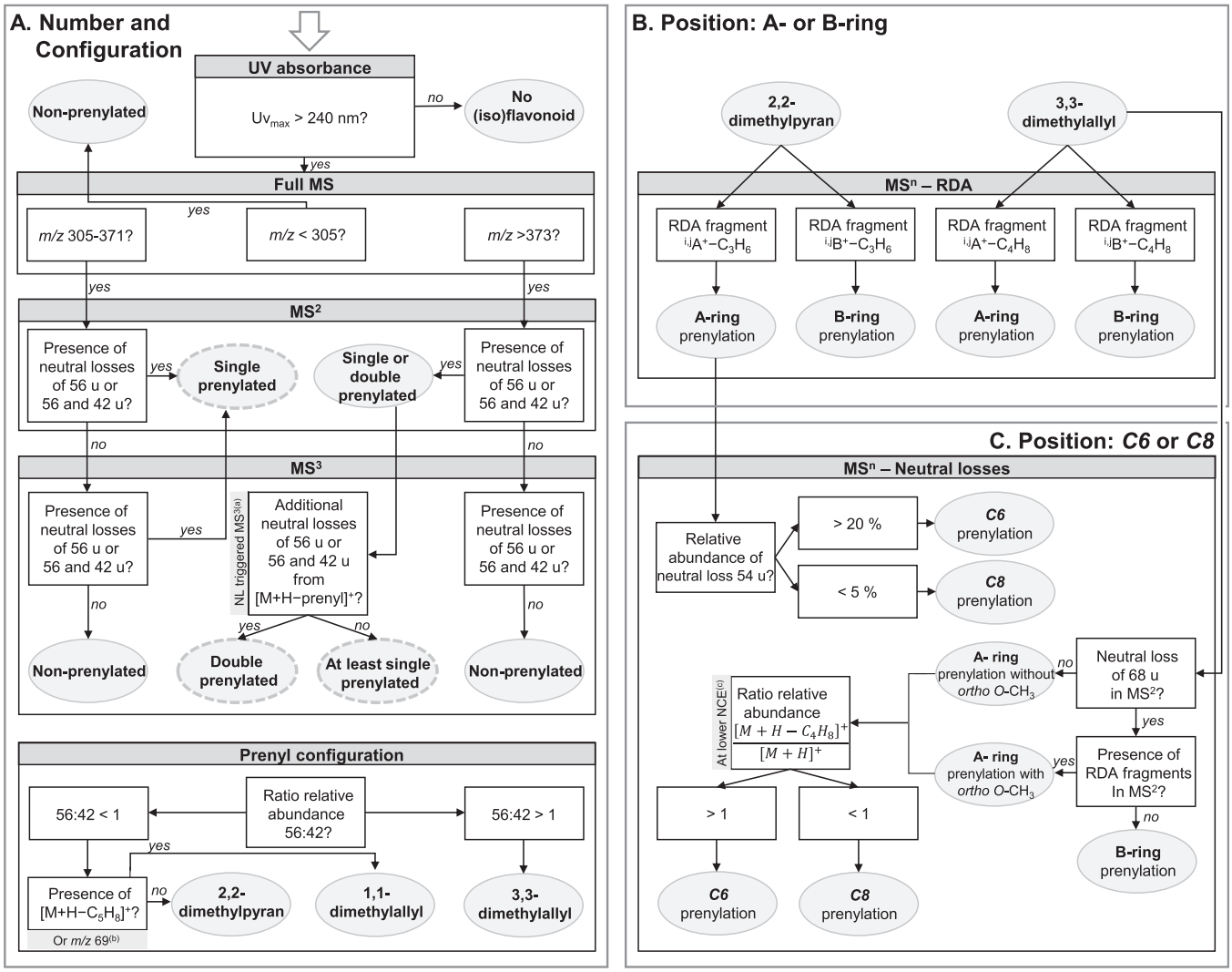

Fig. 5. Decision guideline for annotation of (**A**) prenyl number and configuration, (**B**) A- or B-ring prenylation of 3,3-dimethylallyl and 2,2-dimethylpyran prenylated (iso)flavonoids, and (**C**) *C6* or *C8* prenylation of 3,3-dimethylallyl and 2,2-dimethylpyran prenylated (iso)flavonoids using ESI-IT-MS with CID fragmentation at NCE 35. Prenyl configuration of dashed circles in (**A**) can be determined in box "prenyl configuration". [(a)] Neutral losses of 56 and/or 42 u from fragmentation of the second prenyl can be obtained by neutral loss triggered IT-MS^3 of $[M+H-42]^+$ and/or $[M+H-56]^+$; [(b)] *m/z* 69 cannot be observed in standard CID due to the 1/3rd rule, but is observed when lowering activation Q in CID or in HCD fragmentation, [(c)] Differentiation of relative abundances of ions corresponding to $[M+H-C_4H_8]^+/[M+H]^+$ was achieved by lowering NCE to 20. NL = neutral loss.

second criterion is faced, based on the *m/z* ratio of the parent molecule (Fig. 5A, "full MS"). Our decision guideline does not take into account *O*- or *C*-glycosylated prenylated (iso)flavonoids. For guidelines on identification of *O*- or *C*-glycosides, we refer to work by Vukics and co-workers [45] and Pilon et al. [8] that discuss identification of flavonoid glycosides by mass spectrometry. However, we do not expect that glycosylation affects our guideline (besides changing the *m/z* of parent ion), as sugar moieties are easily cleaved in IT-MS^2 and identified with characteristic neutral losses associated with the glycoside; Jin and co-workers showed that ESI-FT-MS^2 fragmentation (with a CID of 35%) in PI mode of prenylated and glycosylated flavonols yielded fragments $[M+H-sugar]^+$, but also $[M+H-C_4H_8]^+$ [46]. Prenylation (the third criterion in our decision guideline) is confirmed based on detection of NLs of 42 and 56 u in PI mode with IT-MS^2 and MS^3 (Fig. 5A, "MS^2", "MS^3"); a ratio 56:42 >1 indicates 3,3-DMA prenylation and a ratio 56:42 <1 2,2-DMP prenylation (Fig. 5A, "prenyl configuration").

If NLs 42 and 56 u are not present in IT-MS^2 and MS^3 the compound is considered as non-prenylated. Specific for double prenylated molecules is the presence of fragment $[M+H-prenyl-prenyl]^+$ in IT-MS^3, in which the prenyl is either C_3H_6 (42 u) or C_4H_8 (56 u). It should be noted that double prenylation can only be confirmed when the MS^3 fragmentation is performed on the MS^2 ion $[M+H-prenyl]^+$ (*i.e.* $[M+H-C_3H_6]^+$ or $[M+H-C_4H_8]^+$), *e.g.* by applying NL triggered IT-MS^3 on $[M+H-C_3H_6]^+$ and/or $[M+H-C_4H_8]^+$. Our decision guideline also facilitates identification of prenyl position for single prenylated compounds with 2,2-DMP prenylation and compounds with 3,3-DMA prenylation (Fig. 5B and C). The golden standard for identifying A- or B-ring prenylation based on MS is analysis of the RDA fragments in IT-MS^n; fragment $^{i,j}A^+-C_3H_6$ or $^{i,j}B^+-C_3H_6$ confirms 2,2-DMP ring prenylation and fragment $^{i,j}A^+-C_4H_8$ or $^{i,j}B^+-C_4H_8$ confirms 3,3-DMA chain prenylation (Fig. 5B). Additionally, for 3,3-DMA prenylated compounds, a NL of 68 u ($[M+H-C_5H_8]^+$) in combination with absence of RDA fragments in IT-MS^2 indicates B-ring prenylation (Fig. 5C). With respect to 2,2-DMP ring prenylation on the A-ring (*i.e. C6* or *C8*), the ion that corresponds to a NL of 54 u in IT-MS^n with a relative abundance >20% indicates *C6* prenylation, whereas a relative abundance <5% indicates *C8* 2,2-DMP prenylation (Fig. 5C). A relative abundance between 5 and 20% results in an inconclusive outcome. As for the position of 3,3-DMA prenylation on the A-ring, the ratio of relative abundances of ions $[M+H-C_4H_8]^+$ and $[M+H]^+$ in MS^2 identify prenyl position (at lower NCE); $[M+H]^+ < [M+H-C_4H_8]^+$ indicates *C6* prenylation, whereas $[M+H]^+ > [M+H-C_4H_8]^+$ *C8* prenylation (Fig. 5C). It should be noted that identification of *C6* or *C8* prenylation based on MS fragmentation is only possible for single prenylated compounds. We validated our decision guideline with reported spectral data of standards from literature, which is shown in Table S4 (validation of decision guideline).

To summarize, the entirety of our proposed decision guideline can be used with IT-CID-MS, the majority can be used with FT-HCD-MS (an exception is identification of prenyl configuration, which was found to be instrument dependent, section 3.1.2), and at least part of it is applicable to Q-TOF-MS (validation of decision guideline, Table S4). The full range of the guideline's applicability should be further evaluated in the future by analyses on a wider variety of mass spectrometers.

3.3. Annotation and quantification of prenylated (iso)flavonoids in extracts of G. glabra roots

The chromatographic UV profile of EtOAc extract *G. glabra* roots is shown in Fig. 6A. In total, 33 peaks were selected, based on (1) a cut-off that the peak should account for at least 1% of the total UV area at 280 nm and (corresponding to 69% of total UV) (2) compounds that were tentatively identified previously in *G. glabra* extracts at our laboratory [20,28]. Using the established fragmentation behavior of different classes of (iso)flavonoids and the prenylation decision guideline (Fig. 5), the 33 chromatographic UV peaks (representing 36 compounds due to co-elution of compounds) were annotated. Separation on RP-UHPLC was used in combination with IT-MS^n and FT-MS for high resolution mass

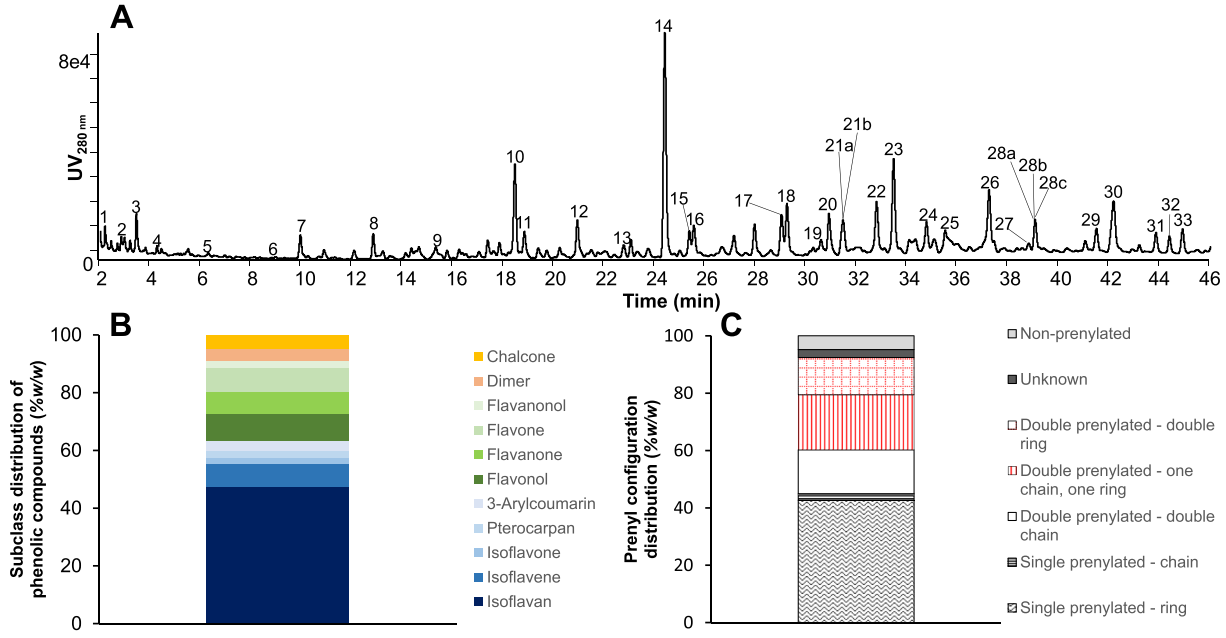

Fig. 6. (**A**) RP-UHPLC-PDA chromatogram (at 280 nm) of EtOAc extract of *Glycyrrhiza glabra* root. Peaks labelled with a number indicate (tentatively) identified phenolic compounds (Table S5, Supplementary Information). (**B**) Distribution of (iso)flavonoid subclasses in EtOAc extract of *G. glabra* root, and (**C**) prenyl configuration (chain = 3,3-dimethylallyl, ring = 2,2-dimethylpyran) of prenylated (iso)flavonoids identified in EtOAc extract of *G. glabra* roots.

determination. UV–Vis absorbance was used to determine (iso) flavonoid subclass. Annotations are listed in Table S5. Proposed fragmentation schemes in PI mode (with FT-MS^n) are shown in Figs. S6–S10. The total content of annotated compounds in the EtOAc extract of *G. glabra* roots was 5.8±0.4 mg g^{-1} DW, of which 5.0±0.4 mg g^{-1} DW were prenylated (iso)flavonoids. Content of each individual compound is given in Table S6. To date, no literature is available on prenylated phenolic content in EtOAc extract of *G. glabra* roots. Nevertheless, in a MeOH extract of *G. glabra* roots, Cheel and co-workers [47] reported total phenolic and total flavonoid content between 72 and 108 mg g^{-1} DW and 18–44 mg g^{-1} DW, respectively [18,47,48]. This higher content is explained by the higher polarity of MeOH compared to EtOAc, leading to extraction of a wider range of non-flavonoid phenolics and non-prenylated flavonoids.

Glabridin content in *G. glabra* roots was 1.00±0.068 mg g^{-1} DW (Table S6), which is in accordance with reported glabridin content ranging between 0.80 and 8 mg g^{-1} DW [49,50]. The majority of annotated peaks in *G. glabra* root extract belonged to the isoflavonoids (67% (*w/w*)) (Fig. 6B). With respect to subclasses, isoflavans represented the majority of the isoflavonoids with 48% (*w/w*) of the total flavonoid content, followed by flavonols and flavanones (flavonoids) with 9% each (*w/w*). Further analysis focused on prenylation showed that double prenylated and single prenylated compounds were equally present with 48% and 45%, respectively (Fig. 6C). Regarding prenyl configuration (3,3-DMA and 2,2-DMP), the majority of single prenylated compounds were 2,2-DMP prenylated (95% of total single prenylated compounds). Double prenylated compounds with one 3,3-DMA and one 2,2-DMP (*e.g.* hispaglabridin A) were most abundant (40% of total double prenylated compounds).

3.4. Screening for prenylation in G. glabra root extract

To apply the decision guideline for prenylation (Fig. 5), the EtOAc extract of *G. glabra* roots was screened for the presence of prenylated (iso)flavonoids in addition to the tentatively annotated compounds (Table S5). This screening was based on screening of the IT-MS^2 and MS^3 chromatograms for presence of NLs of 56 and 42 u. Additionally, we performed NL triggered IT-MS^3 on the ions that corresponded to $[M+H-42]^+$ and $[M+H-56]^+$ in order to identify double prenylation. In total, 209 peaks were selected based on this NL screening (Table S7), thus revealing a wide variety of possible prenylated compounds that were present <1% abundance. All peaks showed an UV absorbance >240 nm. By following our decision guideline, 13 of these peaks were assigned as non-prenylated (m/z < 305 u).

Of the resulting 196 peaks, 75 peaks were assigned as single prenylated and 104 peaks were assigned as double prenylated. The remaining 17 peaks were most likely double prenylated, of which 4 peaks were at least single chain prenylated, 7 peaks at least single ring prenylated, and for 6 peaks no definite prenyl configuration could be determined (Table S7). Regarding single prenylated compounds, 50 peaks were assigned as chain prenylated and 25 peaks as ring prenylated. For the double prenylated compounds, 69 peaks were assigned as double chain prenylated, 32 peaks as ring and chain prenylated, two peaks as double ring prenylated, and one peak was at least single ring prenylated (Tables S7 and S146); the ratio of relative abundances of NLs 56 and 42 u in IT-MS^3 was 1, leading to an inconclusive outcome.

The distribution of prenyl configuration in all 209 compounds annotated based on this screening is visualized in Fig. S5. We compared this distribution with the distribution observed in the main peaks observed in the extract, which were annotated and quantified (section 3.3, Fig. 6C). Based on this, we concluded that the distribution of prenyl configurations found via these two analytical approaches was generally quite comparable; by using our prenylation guideline, fast screening of prenyl configuration without laborious annotation of compounds gives a reasonably accurate representation of prenyl configuration.

To conclude, by applying our decision guideline for prenyl configuration (Fig. 5A), we rapidly identified 196 prenylated compounds in crude EtOAc extract of *G. glabra* roots. This indicates that many more unique prenylated compounds are present in *G. glabra* roots than the ~75 that have been annotated so far [18,51,52]. To develop a full picture that also includes identification of prenyl position, we propose that further work is required regarding automation of our decision guideline; this will facilitate fast identification of prenyl number, configuration, and position in complex plant extracts.

4. Conclusion

In this study, we developed a widely applicable decision guideline that enables identification and characterization of prenylated (iso)flavonoids from different subclasses in complex crude plant extracts. We systematically analyzed fragmentation of prenylated (iso)flavonoids using a combination of IT-MS^n with CID fragmentation and high resolution FT-MS with HCD fragmentation in PI mode. Based on this systematic analysis, we elucidated fragmentation pathways and characteristic spectral features of different subclasses of prenylated (iso)flavonoids, as well as fragmentation patterns and corresponding NLs that resulted in development of an annotation guideline. Whereas previous annotation guidelines only facilitated identification of prenyl configuration, our new guideline allows identification of (i) the presence of an (iso)flavonoid backbone, (ii) prenyl number, (iii) prenyl configuration, and (iv) prenyl position, in complex plant extracts by ESI-IT-MS. Moreover, high resolution MS with HCD fragmentation was used to confirm molecular formulas of fragments and led to the new insights, which uncovered inconsistencies in previously proposed annotation guidelines. Structural characteristics were annotated based on: (i) UV absorbance; (ii) the m/z ratio of the parent compound; (iii) the ratio of relative abundances between NLs 42 and 56 u in MS^n; and (iv) RDA fragments, NLs of 54 and 68 u, and the ratio $[M+H-C_4H_8]^+/[M+H]^+$ in MS^n. With this guideline, we tentatively identified 196 prenylated (iso)flavonoids in *G. glabra* root extract. Prenylated (iso)flavonoid content in the EtOAc extract of *G. glabra* roots was calculated at 5.0±0.4 mg g^{-1} DW *G. glabra* roots.

CRediT authorship contribution statement

Sarah van Dinteren: Conceptualization, Methodology, Investigation, Visualization, Writing – original draft, preparation. **Carla Araya-Cloutier:** Conceptualization, Methodology, Writing – review & editing, Supervision. **Wouter J.C. de Bruijn:** Conceptualization, Methodology, Writing – review & editing. **Jean-Paul Vincken:** Writing – review & editing, Supervision.

Declaration of competing interest

The authors declare that they have no known competing financial interests or personal relationships that could have appeared to influence the work reported in this paper.

Acknowledgements

This work was supported by Topconsortium voor Kennis en Innovatie (TKI, grant number TKI-AF-18124).

Appendix A. Supplementary data

Supplementary data to this article can be found online at https://doi.org/10.1016/j.aca.2021.338874.

References

[1] F. Cuyckens, M. Claeys, Mass spectrometry in the structural analysis of flavonoids, J. Mass Spectrom. 39 (1) (2004) 1–15.
[2] N. Fabre, et al., Determination of flavone, flavonol, and flavanone aglycones by negative ion liquid chromatography electrospray ion trap mass spectrometry, J. Am. Soc. Mass Spectrom. 12 (6) (2001) 707–715.
[3] Y.L. Ma, et al., Characterization of flavone and flavonol aglycones by collision-induced dissociation tandem mass spectrometry, Rapid Commun. Mass Spectrom. 11 (12) (1997) 1357–1364.
[4] R. Maul, N.H. Schebb, S.E. Kulling, Application of lc and gc hyphenated with mass spectrometry as tool for characterization of unknown derivatives of isoflavonoids, Anal. Bioanal. Chem. 391 (1) (2008) 239–250.
[5] J.L. Wolfender, et al., Accelerating metabolite identification in natural product research: toward an ideal combination of liquid chromatography-high-resolution tandem mass spectrometry and NMR profiling, in silico databases, and chemometrics, Anal. Chem. 91 (1) (2019) 704–742.
[6] C. Seger, S. Sturm, H. Stuppner, Mass spectrometry and NMR spectroscopy: modern high-end detectors for high resolution separation techniques - state of the art in natural product HPLC-MS, HPLC-NMR, and CE-MS hyphenations, Nat. Prod. Rep. 30 (7) (2013) 970–987.
[7] J.J.J. van der Hooft, et al., Polyphenol identification based on systematic and robust high-resolution accurate mass spectrometry fragmentation, Anal. Chem. 83 (1) (2011) 409–416.
[8] A.C. Pilon, et al., Mass spectral similarity networking and gas-phase fragmentation reactions in the structural analysis of flavonoid glycoconjugates, Anal. Chem. 91 (16) (2019) 10413–10423.
[9] M.L. Zhang, J.H. Sun, P. Chen, Development of a comprehensive flavonoid analysis computational tool for ultrahigh-performance liquid chromatography-diode array detection-high-resolution accurate mass-mass spectrometry data, Anal. Chem. 89 (14) (2017) 7388–7397.
[10] B. Botta, et al., Prenylated isoflavonoids: botanical distribution, structures, biological activities and biotechnological studies. An update (1995-2006), Curr. Med. Chem. 16 (26) (2009) 3414–3468.
[11] S.K. Chang, Y.M. Jiang, B. Yang, An update of prenylated phenolics: food sources, chemistry and health benefits, Trends Food Sci. Technol. 108 (2021) 197–213.
[12] C.M.M. Santos, A.M.S. Silva, The antioxidant activity of prenylflavonoids, Molecules 25 (3) (2020).
[13] C. Araya-Cloutier, et al., QSAR-based molecular signatures of prenylated (iso) flavonoids underlying antimicrobial potency against and membrane-disruption in gram positive and gram negative bacteria, Sci. Rep. 8 (2018).
[14] D. Barron, R.K. Ibrahim, Isoprenylated flavonoids - A survey, Phytochemistry 43 (5) (1996) 921–982.
[15] K. Šmejkal, Cytotoxic potential of C-prenylated flavonoids, Phytochemistry Rev. 13 (1) (2014) 245–275.
[16] S. Tahara, R.K. Ibrahim, Prenylated isoflavonoids - an update, Phytochemistry 38 (5) (1995) 1073–1094.
[17] X.M. Yang, et al., Prenylated flavonoids, promising nutraceuticals with impressive biological activities, Trends Food Sci. Technol. 44 (1) (2015) 93–104.
[18] W. Song, et al., Biosynthesis-based quantitative analysis of 151 secondary metabolites of licorice to differentiate medicinal Glycyrrhiza species and their hybrids, Anal. Chem. 89 (5) (2017) 3146–3153.
[19] M. Ganzera, S. Sturm, Recent advances on hplc/ms in medicinal plant analysis-an update covering 2011-2016, J. Pharmaceut. Biomed. Anal. 147 (2018) 211–233.
[20] R. Simons, et al., A rapid screening method for prenylated flavonoids with ultra-high-performance liquid chromatography/electrospray ionisation mass spectrometry in licorice root extracts, Rapid Commun. Mass Spectrom. 23 (19) (2009) 3083–3093.
[21] S. Aisyah, et al., Compositional changes in (iso)flavonoids and estrogenic activity of three edible lupinus species by germination and rhizopus-elicitation, Phytochemistry 122 (2016) 65–75.
[22] Y. Wang, et al., Characterization of fifty-one flavonoids in a Chinese herbal prescription longdan xiegan decoction by high-performance liquid chromatography coupled to electrospray ionization tandem mass spectrometry and photodiode array detection, Rapid Commun. Mass Spectrom. 22 (12) (2008) 1767–1778.
[23] S.Q. Fang, et al., Structural characterization and identification of flavonoid aglycones in three Glycyrrhiza species by liquid chromatography with photodiode array detection and quadrupole time-of-flight mass spectrometry, J. Separ. Sci. 39 (11) (2016) 2068–2078.
[24] M.J. Xu, et al., Simultaneous characterization of prenylated flavonoids and isoflavonoids in Psoralea corylifolia l. by liquid chromatography with diode-array detection and quadrupole time-of-flight mass spectrometry, Rapid Commun. Mass Spectrom. 26 (19) (2012) 2343–2358.
[25] Y.F. Zhang, P. Zhang, Y.Y. Cheng, Structural characterization of isoprenylated flavonoids from Kushen by electrospray ionization multistage tandem mass spectrometry, J. Mass Spectrom. 43 (10) (2008) 1421–1431.
[26] M.G.M. van de Schans, et al., Glyceollins and dehydroglyceollins isolated from soybean act as SERMs and ER subtype-selective phytoestrogens, J. Steroid Biochem. Mol. Biol. 156 (2016) 53–63.
[27] C. Araya-Cloutier, et al., The position of prenylation of isoflavonoids and stilbenoids from legumes (Fabaceae) modulates the antimicrobial activity against gram positive pathogens, Food Chem. 226 (2017) 193–201.
[28] M.G.M. van de Schans, et al., Involvement of a hydrophobic pocket and helix 11 in determining the modes of action of prenylated flavonoids and isoflavonoids in the human estrogen receptor, Chembiochem 16 (18) (2015) 2668–2677.
[29] R.S. Burden, J.A. Bailey, G.W. Dawson, Structures of three new isoflavanoids from Phaseolus vulgaris infected with tobacco necrosis virus, Tetrahedron Lett. (41) (1972), p. 4175-+.
[30] S. Kalli, et al., Enhanced biosynthesis of the natural antimicrobial glyceollins in soybean seedlings by priming and elicitation, Food Chem. (2020) 317.
[31] C.A. Williams, J.B. Harborne, Isoflavonoids, in: Methods in Plant Biochemistry, Elsevier, 1989, pp. 421–449.
[32] W.Z. Yang, et al., Collision-induced dissociation of 40 flavonoid aglycones and differentiation of the common flavonoid subtypes using electrospray ionization ion-trap tandem mass spectrometry and quadrupole time-of-flight mass spectrometry, Eur. J. Mass Spectrom. 18 (6) (2012) 493–503.
[33] T. Fossen, Ø.M. Andersen, Spectroscopic techniques applied to flavonoids, in: Flavonoids, CRC press, 2005, pp. 48–153.
[34] K.R. Markham, T. Mabry, Ultraviolet-visible and proton magnetic resonance spectroscopy of flavonoids, in: The Flavonoids, Springer, 1975, pp. 45–77.
[35] A.F. Magalhães, et al., Flavonoids of Lonchocarpus montanus a.M.G. Azevedo and biological activity, An Acad. Bras Ciências 79 (3) (2007) 351–367.
[36] Y.R. Lee, D.H. Kim, A new route to the synthesis of pyranoflavone and pyranochalcone natural products and their derivatives, Synthesis (4) (2006) 603–608.
[37] D.P. Demarque, et al., Fragmentation reactions using electrospray ionization mass spectrometry: an important tool for the structural elucidation and characterization of synthetic and natural products, Nat. Prod. Rep. 33 (3) (2016) 432–455.
[38] M. George, et al., Gas-phase nazarov cyclization of protonated 2-methoxy and 2-hydroxychalcone: an example of intramolecular proton-transport catalysis, J. Am. Soc. Mass Spectrom. 20 (5) (2009) 805–818.
[39] L.Y. Huang, D. Nikolic, R.B. van Breemen, Hepatic metabolism of licochalcone A, a potential chemopreventive chalcone from licorice (Glycyrrhiza inflata), determined using liquid chromatography-tandem mass spectrometry, Anal. Bioanal. Chem. 409 (30) (2017) 6937–6948.
[40] C. Lössner, W. Blackstock, J. Gunaratne, Enhanced performance of pulsed Q collision induced dissociation-based peptide identification on a dual-pressure linear ion trap, J. Am. Soc. Mass Spectrom. 23 (1) (2012) 186–189.
[41] R. Simons, et al., Identification of prenylated pterocarpans and other isoflavonoids in Rhizopus spp. elicited soya bean seedlings by electrospray ionisation mass spectrometry, Rapid Commun. Mass Spectrom. 25 (1) (2011) 55–65.
[42] A.K. Waffo, et al., Indicanines B and C, two isoflavonoid derivatives from the root bark of Erythrina indica, Phytochemistry 53 (8) (2000) 981–985.
[43] J.F. Stevens, et al., Prenylflavonoids from Humulus lupulus, Phytochemistry 44 (8) (1997) 1575–1585.
[44] M. Takayama, et al., Mass spectrometry of prenylated flavonoids, Heterocycles 33 (1) (1992) 405–434.
[45] V. Vukics, A. Guttman, Structural characterization of flavonoid glycosides by multi-stage mass spectrometry, Mass Spectrom. Rev. 29 (1) (2010) 1–16.
[46] Y. Jin, et al., A new strategy for the discovery of Epimedium metabolites using high-performance liquid chromatography with high resolution mass spectrometry, Anal. Chim. Acta 768 (2013) 111–117.
[47] J. Cheel, et al., Variations in the chemical profile and biological activities of licorice (Glycyrrhiza glabra l.), as influenced by harvest times, Acta Physiol. Plant. 35 (4) (2013) 1337–1349.
[48] T.K. Lim, Glycyrrhiza glabra, in: Edible Medicinal and Non-medicinal Plants, Springer, 2016, pp. 354–457.
[49] H. Hayashi, et al., Field survey of Glycyrrhiza plants in central Asia (3). Chemical characterization of G. glabra collected in Uzbekistan, Chem. Pharmaceut. Bull. 51 (11) (2003) 1338–1340.
[50] K. Shanker, et al., RP-HPLC method for the quantitation of glabridin in yashtimadhu (Glycyrrhiza glabra), Chromatographia 65 (11–12) (2007) 771–774.
[51] A.S. Ammosov, V.I. Litvinenko, Phenolic compounds of the genera Glycyrrhiza l. and meristotropis fisch et mey. (review), Pharmaceut. Chem. J. 41 (7) (2007) 372–395.
[52] T. Nomura, T. Fukai, Phenolic constituents of licorice (Glycyrrhiza species), in: Fortschritte der chemie organischer naturstoffe/progress in the chemistry of organic natural products, Springer, 1998, pp. 1–140.